# Conjugated Donor−Acceptor Copolymer Semiconductors. Synthesis, Optical Properties, Electrochemistry, and Field-Effect Carrier Mobility of Pyridopyrazine-Based Copolymers

**Pei-Tzu Wu, Felix S. Kim, Richard D. Champion, and Samson A. Jenekhe***

*Departments of Chemical Engineering and of Chemistry, University of Washington, Seattle, Washington 98195-1750*

*Received June 15, 2008; Revised Manuscript Received August 2, 2008*

ABSTRACT: Five conjugated pyrido[3,4-*b*]pyrazine-based donor−acceptor copolymers were synthesized by Suzuki and Stille coupling polymerizations, and their photophysical and electrochemical properties and field-effect carrier mobilities were characterized. The copolymer semiconductors include poly(pyrido[3,4-*b*]pyrazine-*alt*-9,9-dioctyl-2,7-fluorene) (PPPzF), poly(thiophene-2,5-diyl-*alt*-2,3-diheptyl-pyrido[3,4-*b*]pyrazine-5,8-diyl) (PTHPPz), poly(thiophene-2,5-diyl-*alt*-2,3-didecyl-pyrido[3,4-*b*]pyrazine-5,8-diyl) (PTDPPz), poly(5,8-bis(4-dodecyl-thiophen-2-yl)-2,3-dioctyl-pyrido[3,4-*b*]pyrazine-*alt*-2,5-thiophene) (P3TPPz), and poly(5,8-bis(4-dodecyl-thiophen-2-yl)-2,3-dioctyl-pyrido[3,4-*b*]pyrazine-*alt*-9,9-dioctyl-2,7-fluorene) (P2TPPzF). Those soluble in tetrahydrofuran have moderate weight-average molecular weights (19 700−70 400 g/mol). The copolymers have tunable optical absorption bands in the visible region with absorption maxima at 323−588 nm and optical band gaps of 1.75−2.48 eV. Ambipolar redox properties with ionization potentials at 5.20−5.68 eV and electron affinities at 2.86−3.02 eV were observed by cyclic voltammetry. Field-effect hole mobilities of $4.1 \times 10^{-4}$−$4.4 \times 10^{-3}$ $cm^2/(V\ s)$ were observed in PTHPPz, PTDPPz, and P3TPPz copolymers. The combination of ambipolar redox properties and visible region broad absorption bands with fairly high carrier mobilities observed in pyrido[3,4-*b*]pyrazine-based donor−acceptor copolymer semiconductors make them promising materials for organic electronic and optoelectronic devices.

## Introduction

Conjugated donor−acceptor (D−A) copolymer semiconductors are of growing interest for organic optoelectronic and electronic applications,[1–5] including photovoltaic cells,[3] light-emitting diodes (LEDs),[4] and field-effect transistors (FETs).[5] Thiophene-based alternating D−A copolymers have been of particular recent interest because intramolecular charge transfer (ICT) interaction between the thiophene donor moieties and electron acceptor units within the D−A copolymers can be readily tailored to modulate their electronic structures (HOMO/LUMO levels) and electronic and optoelectronic properties.[1–5]

Many electron acceptors, including quinoline,[1e,2] quinoxaline,[2d,4b,5b] 2,1,3-benzothiadiazole,[3f] thiazole,[5e] 1,3,4-thiadiazole,[5d] pyridazine,[5g] and 1,3,5-triazine,[5i] have been explored in constructing $\pi$-conjugated D−A copolymer systems. However, the electron-accepting properties of most of these acceptors, and thus the strength of the ICT in the associated D−A copolymers, are only strong enough to generate absorption bands in the visible region. A few strong electron acceptors, such as thieno[3,4-*b*]pyrazine,[3d,e,4d] [1,2,5]thiadiazolo[3,4-*g*]quinoxaline,[5f] and pyrazino[2,3-*g*]quinoxaline,[2e] have been incorporated into conjugated D−A copolymers, resulting in very small band gaps. However, the charge carrier transport properties of conjugated D−A copolymers remain to be fully investigated. The hole mobility and charge carrier transport in thiophene−quinoxaline and thiophene−thienopyrazine copolymers were recently reported by our group.[5a,b] As clearly demonstrated with regioregular poly(3-hexylthiophene), the charge carrier mobility of polymer semiconductors strongly depends on molecular weight.[6] One challenge toward higher carrier mobilities is to achieve high molecular weight D−A copolymers. Yet, another challenge is to obtain high molecular weight conjugated copolymers and still maintain good solubility in organic solvents to facilitate thin film processing.

* Author for all correspondence. E-mail: jenekhe@u.washington.edu.

Pyrido[3,4-*b*]pyrazine ring has previously been incorporated into poly(phenylenevinylene)s used as an electron acceptor with poly(2-methoxy-5-(2′-ethylhexyloxy)-1,4-phenylenevinylene) (MEH-PPV) as an electron donor in photodiodes and solar cell application.[7a] Another poly(pyridopyrazine vinylene) copolymer, including the pyrido[3,4-*b*]pyrazine acceptor, was synthesized, and its use in near-infrared LEDs was demonstrated.[4e] It is to be noted that low molecular weights ($<10^4$ g/mol) were observed in those poly(pyridopyrazine vinylene)s.[4e,7b] Alternating pyridopyrazine−thiophene copolymers were found to exhibit interesting absorption and redox properties.[1b] However, the copolymers were only soluble in acidic solvents (formic acid and trifluoroacetic acid),[1b] and field-effect charge transport of such alternating pyridopyrazine−thiophene copolymers has not been reported.[1b] Very recently, a carbazole-containing D−A copolymer with pyrido[3,4-*b*]pyrazine acceptor was shown to exhibit a hole mobility of $2 \times 10^{-5}$ $cm^2/(V\ s)$,[3i] while our work was in progress.

In a related earlier work, the synthesis and thin film transistor properties of thienopyrazine-based D−A copolymers were reported.[5a] In this paper, we report the synthesis, electrochemical and photophysical properties, and the field-effect carrier mobility of a series of soluble donor−acceptor copolymer semiconductors based on pyrido[3,4-*b*]pyrazine as the electron-accepting building block. Five conjugated copolymers were synthesized by Stille or Suzuki coupling polymerization and investigated, including poly(pyrido[3,4-*b*]pyrazine-*alt*-9,9-dioctyl-2,7-fluorene) (PPPzF), poly(thiophene-2,5-diyl-*alt*-2,3-diheptylpyrido[3,4-*b*]pyrazine-5,8-diyl) (PTHPPz), poly(thiophene-2,5-diyl-*alt*-2,3-didecylpyrido[3,4-*b*]pyrazine-5,8-diyl) (PTDPPz), poly(5,8-bis(4-dodecylthiophen-2-yl)-2,3-dioctylpyrido[3,4-*b*]pyrazine-*alt*-2,5-thiophene) (P3TPPz), and poly(5,8-bis(4-dodecylthiophen-2-yl)-2,3-dioctylpyrido[3,4-*b*]pyrazine-*alt*-9,9-dioctyl-2,7-fluorene) (P2TPPzF) (Chart 1). PTHPPz and PTDPPz have an alternating acceptor (A)−donor (D) chain structure of the form ···A−D−A−D···, where A is dialkylpyrido[3,4-*b*]pyrazine and

10.1021/ma801348b CCC: $40.75 
Published on Web 09/12/2008

**Chart 1**

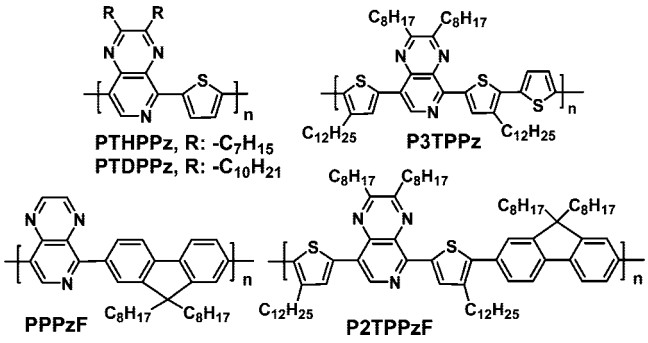


D is 2,5-linked thiophene; P3TPPz has a longer donor block in the alternating main chain (···A−DDD−A−DDD···). The longer alkyl chains are incorporated into PTDPPz and P3TPPz to render better solubility than heptyl chains in PTHPPz. To compare modulation of the ICT strength and thus the electronic and optical properties, PPPzF and P2TPPzF with chain structures of ···A−E−A−E··· and ···DAD−E−DAD−E··· were synthesized, where the moiety E is a dioctylfluorene (weak donor). We show that these D−A copolymers exhibit moderate intramolecular charge transfer, have optical band gaps (1.75−2.48 eV) and broad absorption bands in the visible region, and exhibit ambipolar redox properties with ionization potentials of 5.20−5.68 eV. The D−A copolymers with incorporated long alkyl chains have good solubility as expected, except PTHPPz which is only processable in acidic solvents. Initial organic field-effect transistors (OFETs) made from the copolymer semiconductors showed field-effect hole mobilities of up to $4.4 \times 10^{-3}$ cm$^2$/(V s).

## Results and Discussion

**Synthesis and Characterization.** The synthetic routes to the monomers and polymers are outlined in Scheme 1. The Stille coupling reaction between 5-tributylstannyl-(3-dodecylthiophene) and 5,7-dibromo-2,3-dioctylpyrido[3,4-*b*]pyrazine in the presence of a catalytic amount of $Pd(PPh_3)_4$ afforded compound **1**. Bromination of **1** by *N*-bromosuccinimide (NBS) gave the dibromo monomer **2**. Poly(pyrido[3,4-*b*]pyrazine-*alt*-9,9-dioctyl-2,7-fluorene) (PPPzF) and poly(5,8-bis(4-dodecylthiophen-2-yl)-2,3-dioctylpyrido[3,4-*b*]pyrazine-*alt*-9,9-dioctyl-2,7-fluorene) (P2TPPzF) were synthesized by Suzuki coupling polymerization. Poly(thiophene-2,5-diyl-*alt*-2,3-diheptylpyrido[3,4-*b*]pyrazine-5,8-diyl) (PTHPPz), poly(thiophene-2,5-diyl-*alt*-2,3-didecylpyrido[3,4-*b*]pyrazine-5,8-diyl) (PTDPPz), and poly(5,8-bis(4-dodecyl-thiophen-2-yl)-2,3-dioctylpyrido[3,4-*b*]pyrazine-*alt*-2,5-thiophene) (P3TPPz) were synthesized by Pd(0)-mediated Stille coupling polymerization in toluene. All the copolymers, except PTHPPz, were partially soluble in organic solvents (e.g., chloroform and toluene) at room temperature and completely soluble in high boiling point solvents (e.g., chlorobenzene) at high temperature. PTHPPz was not soluble in most organic solvents probably due to the absence of longer solubilizing groups on the pyrido[3,4-*b*]pyrazine ring. The number-average molecular weights ($M_n$) of P3TPPz, P2TPPzF, and PPPzF were determined by gel permeation chromatography (GPC) against polystyrene standards in tetrahyrdofuran and found to be 10 000−19 800 g/mol with polydispersity index ($M_w/M_n$) of 1.97−3.64 (Table 1). The molecular weights of PTHPPz and PTDPPz could not be determined by GPC because of their poor solubility in tetrahydrofuran. Although the molecular weight of P3TPPz is not very high, it can be increased by optimizing the Stille polymerization condition, such as using different solvents or catalysts.

The molecular structures of the copolymers were verified by FT-IR and $^1$H NMR. FT-IR spectra of the copolymers confirmed their molecular structures. The vibrational bands at 1533−1544 cm$^{-1}$ in all the copolymers are due to stretching vibrations of the C=N group and are characteristic of the pyrido[3,4-*b*]pyrazine ring.[1b] The strong bands at about 1431−1450 cm$^{-1}$ of PTHPPz, PTDPPz, P3TPPz, and P2TPPzF are assigned to the stretching vibrations of α,α′-coupled thiophene rings.

The $^1$H NMR spectra of the copolymers were in good agreement with the proposed structures. The singlet resonance at 9.17 ppm, assigned to the proton adjacent to the imine nitrogen atom of pyridopyrazine unit, was observed in PPPzF. The two resonances at 9.13 and 9.07 ppm are assigned to the two neighboring protons adjacent to the imine nitrogen atoms of pyridopyrazine unit in the spectra of PPPzF. In P2TPPzF and P3TPPz spectra (in $CDCl_3$), the only proton adjacent to the imine nitrogen atom of pyridopyrazine ring was observed as a singlet resonance at 9.07 and 9.12 ppm, respectively. The protons of the two thienyl rings adjacent to pyrido[3,4-*b*]pyrazine moieties showed as two singlet resonances in P3TPPz ($\delta$ 7.78, 8.52 ppm) and P2TPPzF ($\delta$ 7.82, 8.64 ppm); similarly, the two protons of the thienyl rings in PTHPPz and PTDPPz were observed as two singlet resonances at 8.64 and 8.29 ppm due to the asymmetric pyrido[3,4-*b*]pyrazine unit which has three imine nitrogen atoms. These two singlet resonances, indicative of the asymmetric nature of the pyrido[3,4-*b*]pyrazine moieties in the copolymers, had a peak ratio of 1. This means that the pyridopyrazine rings separated by a donor in the backbone have 50% head-to-tail and 50% head-to-head couplings in the copolymers. Resonances at 7.84−8.29 and 7.58−7.80 ppm in the spectra of PPPzF and P2TPPzF are assigned to the protons in the fluorene ring. The proton NMR peaks in the range 0.8−3.53 ppm arise from alkyl groups in the copolymers; the peak area ratio between the aromatic and aliphatic protons in the NMR spectra agrees with the molecular structures of the copolymers.

The thermogravimetric analysis (TGA) scans of the five copolymers are shown in Figure 1. The TGA thermograms revealed that the onset decomposition temperatures of the D−A copolymers under nitrogen flow were in the range of 310−419 °C (Table 1), indicative of good thermal stability. The earlier onset of thermal decomposition of P2TPPzF (200 °C) compared to the other copolymers is possibly because of the low molecular weight fraction in the polymer sample since we noted that it had a broad molecular weight distribution (PDI = 3.64).

**Optical Properties.** The optical absorption spectra of the copolymers in dilute ($10^{-6}$ M) chloroform solution and as thin films are shown in Figure 2. The dilute chloroform solution of each copolymer was filtered (0.45 $\mu$m filter) to remove insoluble residue before the absorption spectrum was obtained. The main optical properties of the D−A copolymers are summarized in Table 2. PPPzF with the weak electron-donating dialkylfluorene moiety (E) was characterized by two absorption bands at 325 and 434 nm in dilute solution (Figure 2A). The former band can be assigned to $\pi-\pi^*$ transition whereas the lowest energy band is due to intramolecular charge transfer (ICT) interactions between the donor and the pyrido[3,4-*b*]pyrazine acceptor moieties. The solution absorption spectrum of P2TPPzF with two absorption maximum ($\lambda_{max}^{abs}$) at 352 and 472 nm are broadened and red-shifted compared to those of PPPzF ($\lambda_{max}^{abs}$ = 325 and 434 nm), which resulted from the strong ICT effects on the D−A−D bridged by the dialkylfluorene unit (E). The ICT absorption bands of PTHPPz and PTDPPz were red-shifted to 517−526 nm due to the stronger electron-donating thiophene moieties. Similarly, the 372 nm band in the absorption spectrum of P3TPPz in dilute solution can be assigned to the $\pi-\pi^*$ transition whereas the 522 nm band originated from strong ICT[1] between the thiophene donor and the pyrido[3,4-*b*]pyrazine acceptor moieties. Among these five copolymers, P3TPPz with

**Scheme 1**

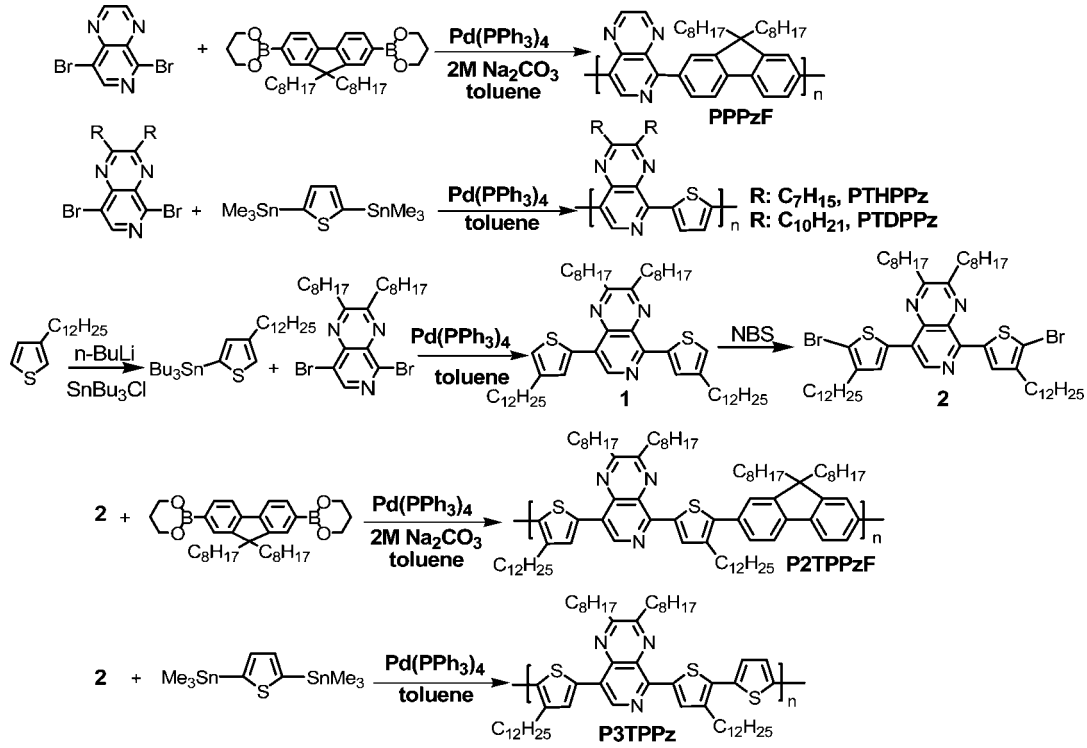


**Table 1. Molecular Weight and Charge Transport Properties of Polymers**

| copolymer | yield (%) | $M_w$[a] | $M_n$[a] | $M_w/M_n$[a] | $T_d$[c] (°C) | $\mu_h$ (cm²/(V s)) | $I_{on/off}$ | $V_T$ (V) |
|---|---|---|---|---|---|---|---|---|
| PPPzF | 81 | 70 400 | 19 800 | 3.56 | 419 | | | |
| PTHPPz | 50 | –[b] | –[b] | –[b] | 382 | $4.1 \times 10^{-4}$ [d] | $10^4$ | −12 |
| PTDPPz | 65 | –[b] | –[b] | –[b] | 383 | $4.4 \times 10^{-3}$ [d] | $10^6$ | −18 |
| P3TPPz | 85 | 19 700 | 10 000 | 1.97 | 405 | $5.8 \times 10^{-4}$ [d] | $10^5$ | −23 |
| P2TPPzF | 25 | 51 300 | 14 100 | 3.64 | 310 | | | |

[a] Molecular weights were determined by GPC using polystyrene standards. [b] Not determined due to the poor solubility in tetrahydrofuran. [c] Onset decomposition temperature measured from TGA under nitrogen. [d] The devices were annealed at 100 °C for 10 min before measurements.

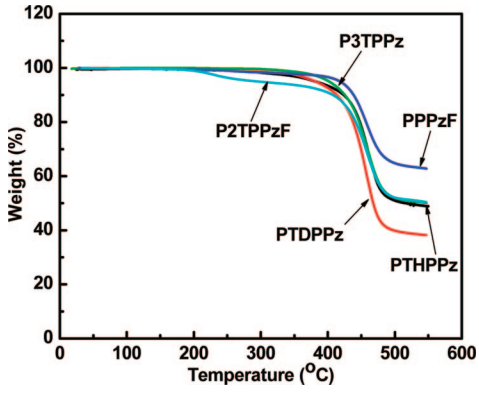


**Figure 1.** TGA thermograms of five pyrido[3,4-*b*]pyrazine-based donor−acceptor copolymers in $N_2$.

alternating ···A−DDD−A−DDD··· chain structure has the highest degree of electronic delocalization. PTHPPz and PTDPPz with a similar alternating ···A−D−A−D··· chain structure still show strong ICT and great delocalization between the single thiophene donor and the pyridopyrazine acceptor. However, in the main-chain structures of PPPzF (···A−E−A−E···) and P2TPPzF (···A−DED−A−DED···), there is a large decrease in the ICT strength and electronic delocalization because the dialkylfluorene moiety (E) is a poorer electron-donating building block compared to the thiophene donor and also due to the significantly lower chain structure symmetry.

Figure 2B shows the optical absorption spectra of thin films of the pyrido[3,4-*b*]pyrazine-based copolymers. The thin film

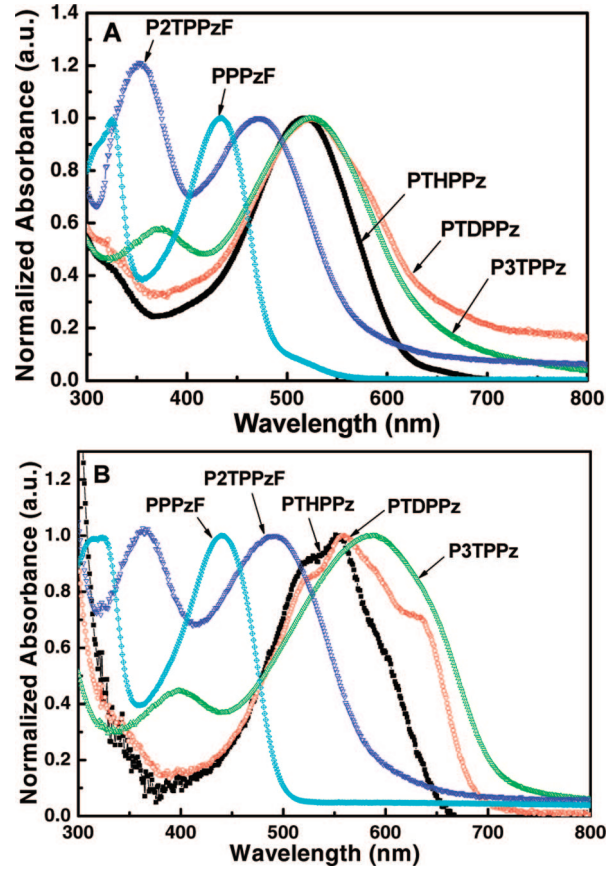


**Figure 2.** Optical absorption spectra of the D−A copolymers in $10^{-6}$ M $CHCl_3$ solutions (A) and as thin films on glass substrates (B).

**Table 2. Optical and Redox Properties of Copolymers**

| | solution | | film | | | | | | | |
|---|---|---|---|---|---|---|---|---|---|---|
| copolymer | $\lambda_{max}^{abs}$ (nm) | $\lambda_{max}^{em}$ (nm) | $\lambda_{max}^{abs}$ (nm) | $\lambda_{max}^{em}$ (nm) | $E_g^{opt}$ (eV) | $E_{ox}^{onset a}$ (V) | IP[b] (eV) | $E_{red}^{onset a}$ (V) | EA[c] (eV) | $E_g^{el}$ (eV) |
| PPPzF | 325, 434 | 536 | 323, 440 | 534 | 2.48 | 1.28 | 5.68 | −1.52 | 2.88 | 2.80 |
| PTHPPz | 517 | 613 | 554 | 667 | 1.89 | 0.89 | 5.29 | −1.54 | 2.86 | 2.43 |
| PTDPPz | 526 | 626 | 560 | 685 | 1.81 | 0.91 | 5.31 | −1.38 | 3.02 | 2.29 |
| P3TPPz | 372, 522 | 661 | 399, 588 | 713 | 1.75 | 0.80 | 5.20 | −1.56 | 2.84 | 2.36 |
| P2TPPzF | 352, 472 | 611 | 363, 492 | 692 | 2.10 | 1.02 | 5.42 | −1.48 | 2.92 | 2.50 |

[a] Onset oxidation and reduction potentials vs SCE. [b] Ionization potential was obtained based on IP = $E_{ox}^{onset}$ + 4.4 eV. [c] Electron affinity was obtained based on EA = $E_{red}^{onset}$ + 4.4 eV.

absorption spectra with two characteristic bands centered at 323−339 and 440−588 nm are generally similar in shape to those in dilute solutions. The absorption maximum of PPPzF and P2TPPzF at 440 and 492 nm are only 6 and 20 nm red-shifted compared to the corresponding spectra in dilute solution. In the case of PTHPPz, PTDPPz, and P3TPPz, their absorption spectra in the solid state exhibit larger red shifts (34−66 nm) in the lowest-energy absorption peaks compared to the corresponding spectra in dilute solutions. The small increase in the electronic delocalization length of the copolymers in the solid state can be explained by their nonplanar conformations due to their long alkyl side chains in the solid state. The ICT absorption band is here shown to be tunable from 440 to 588 nm. The optical band gap ($E_g^{opt}$) derived from the absorption edge of the thin film spectra was in the range of 1.75−2.48 eV (Table 2). As expected, P3TPPz with the strongest intramolecular charge transfer interaction thus has the smallest optical band gap, 1.75 eV, which is 0.25 eV smaller than that of poly(3-alkylthiophene) homopolymer (~2.0 eV).[8] It is evident from these results that the ICT interaction between donor and acceptor moieties in D−A copolymers is a practical approach to lower the band gap of conjugated polymers as already well established.[1,3d–g,i] The tunable optical band gaps and broad absorption bands across the entire visible wavelength region, by tailoring the main-chain structures achieved of these pyrido[3,4-*b*]pyrazine-based copolymer semiconductors, suggest that they could be useful materials for photovoltaic applications.[3]

The normalized photoluminescence (PL) emission spectra of the pyrido[3,4-*b*]pyrazine-based D−A copolymers are shown in Figure 3. PPPzF shows bright green PL emission with a $\lambda_{max}$ at 536 nm in dilute chloroform solution and a broad, featureless emission band at 534 nm in thin film. P2TPPzF has a broad, featureless emission band centered at 611 nm in chloroform solution and at 692 nm in thin film. PTHPPz, PTDPPz, and P3TPPz similarly had broad emission bands with peaks at 613−661 nm in dilute chloroform solutions and very weak emission with $\lambda_{max}$ at 667−713 nm in thin films. Although the broad and featureless emission bands of conjugated thin films are commonly due to aggregation and excimer emission,[9] the weak PL emission of the present donor−acceptor copolymers originates from ICT excited states.[1e]

**Electrochemical Properties.** The electronic states, HOMO/LUMO levels (ionization potential/electronic affinity), of the pyrido[3,4-*b*]pyrazine-based conjugated donor−acceptor copolymers were investigated by cyclic voltammetry (CV). The oxidation and reduction cyclic voltammograms of the copolymer thin films are shown in Figure 4, and all the electrochemical redox data are summarized in Table 2. PTHPPz, PTDPPz, and P3TPPz have reversible oxidation and reversible reduction as evident from the areas and close proximity of the anodic and cathodic peaks in the cyclic voltammograms (CVs). However, PPPzF and P2TPPzF do not show reversible oxidation waves. The formal reduction potentials of the five copolymers are very close at −1.56 to −1.65 V (vs SCE) due to the same pyrido[3,4-*b*]pyrazine unit. The formal oxidation potentials of PTHPPz, PTDPPz, and P3TPPz are in the range of 1.08−1.11 V (vs SCE).

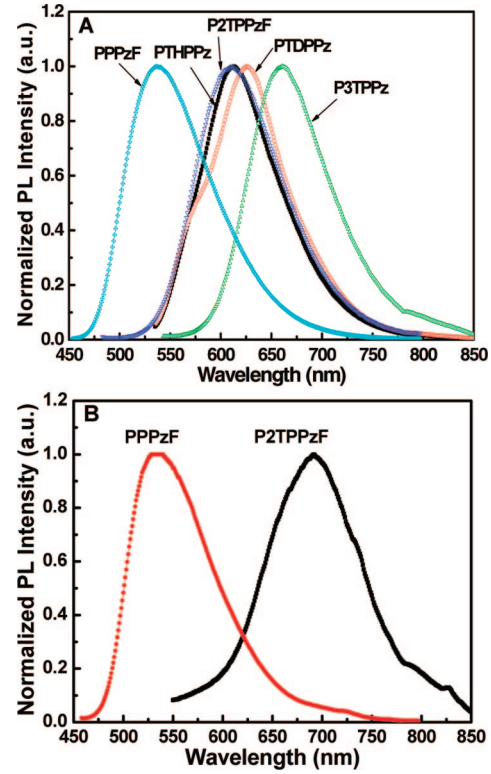


**Figure 3.** PL emission spectra of the D−A copolymers in $10^{-6}$ M $CHCl_3$ solution (A) and as thin films on glass substrates (B).

The onset oxidation potential and onset reduction potential of the copolymer PPPzF are 1.28 and −1.52 V, respectively, from which we estimate an ionization potential (IP, HOMO level) of 5.68 eV (IP = $E_{ox}^{onset}$ + 4.4)[10] and an electron affinity (EA, LUMO level) of 2.88 eV (EA = $E_{red}^{onset}$ + 4.4).[10] The onset oxidation potential and onset reduction potential of the copolymer PTDPPz are 0.91 and −1.38 V, respectively, from which we estimate an IP of 5.31 eV and an EA of 3.02 eV.[10] Similar reversible oxidation and reversible reduction were observed in a pyrido[3,4-*b*]pyrazine−thiophene copolymer in the literature.[1b] The IP and EA values of P2TPPzF were similarly estimated to be 5.42 and 2.92 eV, respectively. The HOMO and LUMO levels of poly(9,9-octylfluorene) (PFO) are known to be 5.6 and 2.0 eV, respectively, when measured under the same conditions. It is clear that the HOMO/LUMO levels of P2TPPzF have been varied relative to those of PFO and PTHPPz/PTDPPz due to the modulation of the ICT strength by the presence of the dialkylfluorene moieties in such ···A−DED−A−DED··· architecture.

The highly reversible electrochemical oxidation and reduction and moderate IP values of PTHPPz, PTDPPz, and P3TPPz suggest potential for efficient hole/electron injection or transport in organic electronic devices. The electrochemical band gap ($E_g^{el}$ = IP − EA) was determined to be 2.29−2.36 eV for PTHPPz, PTDPPz, and P3TPPz; high $E_g^{el}$ of 2.50 and 2.80 eV were derived for P2TPPzF and PPPzF because they have weak ICT

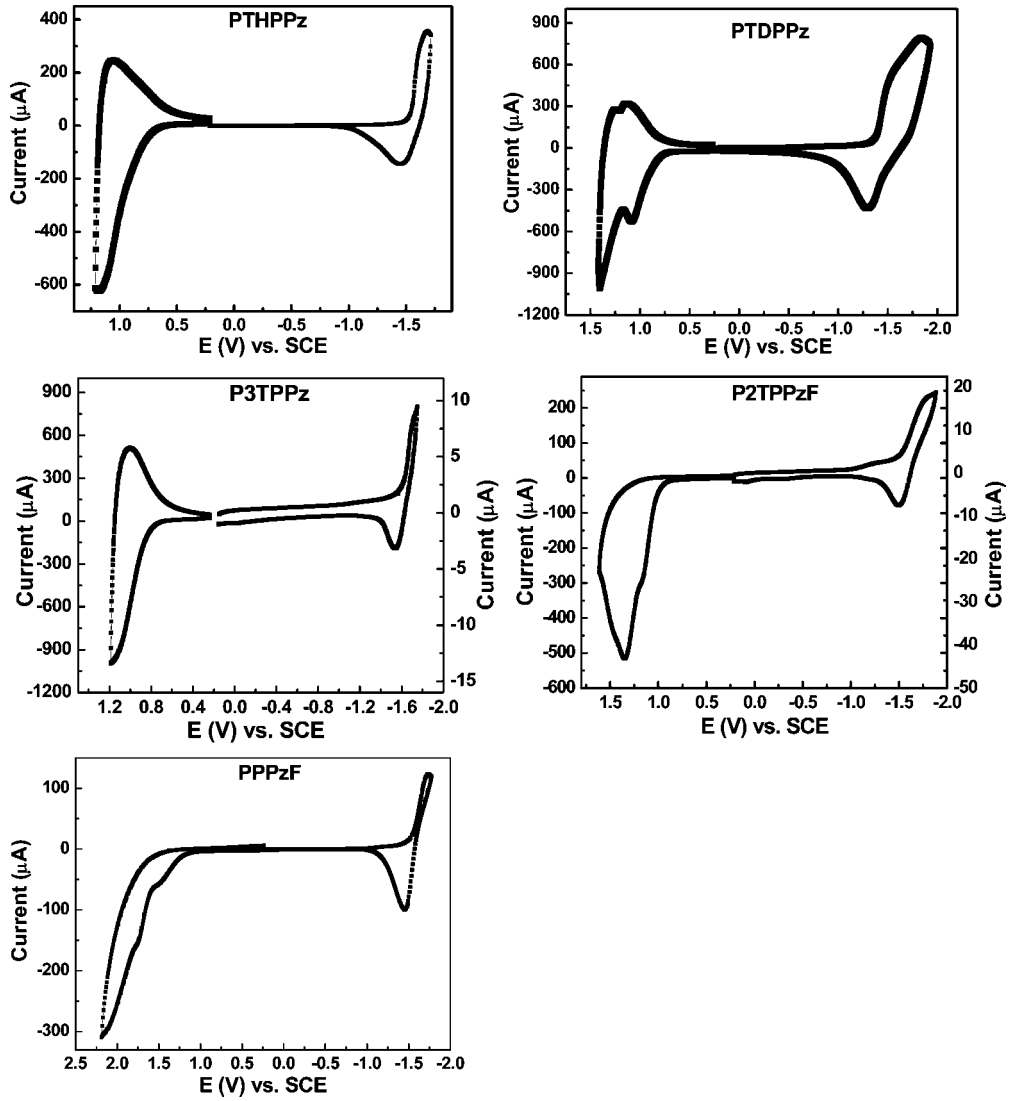


**Figure 4.** Cyclic voltammograms of the D−A copolymer thin films in 0.1 M $Bu_4NPF_6$ solution in acetonitrile at a scan rate of 50 mV/s.

effect and poor electron delocalization due to the presence of dialkylfluorene moieties. Their $E_g^{el}$ are 0.3−0.6 eV larger than the optically determined ones ($E_g^{opt}$ = 1.75−2.48 eV). This difference between optical and electrochemical band gap energies can be explained in part by the exciton binding energy of conjugated polymers which is believed to be in the range of ~0.4−1.0 eV.[11]

**Field-Effect Transistor Characteristics.** The field-effect mobilities of charge carriers in the pyrido[3,4-*b*]pyrazine-based D−A copolymers were investigated by fabricating and evaluating thin film field-effect transistors based on the bottom contact geometry similar to our previous reports.[12a–c] Three of the D−A copolymers showed typical p-channel output characteristics (plot of drain current $I_D$ vs drain voltage $V_D$ at different gate voltages $V_G$) when operated in the accumulation mode.[13] In the saturation region, $I_D$ can be described by the equation[13]

$$I_D = (W/2L)C_0\mu_h(V_G - V_T)^2 \quad (1)$$

where $\mu_h$ is the field-effect hole mobility, $W$ is the channel width, $L$ is the channel length, and $C_0$ is the capacitance per unit area of the gate dielectric layer ($SiO_2$, 300 nm, $C_0$ = 11 nF/cm$^2$), and $V_T$ is the threshold voltage. The saturation region field-effect mobility was thus calculated from the transfer characteristics of the OFETs involving plotting $I_D^{1/2}$ vs $V_G$. To promote the molecular chain ordering of the polymer semiconductor at the gate dielectric/semiconductor interface, the gate dielectric surface was modified by the silane coupling agent octyltrichlorosilane (OTS-8).[14]

PTHPPz thin films, which can only be spin-coated from acidic solvents such as trifluoroacetic acid, gave a saturation region mobility of 4.1 × 10$^{-4}$ cm$^2$/(V s) with an on/off current ratio of 10$^4$ (Table 1). PTDPPz showed a significantly better performance compared to PTHPPz because it has longer solubilizing alkyl chains that allow processing in organic solvent. Figure 5 shows the output and transfer characteristics of a PTDPPz OFET processed from 1,2,4-trichlorobenzene. A field-effect mobility of holes of 4.4 × 10$^{-3}$ cm$^2$/(V s) and an on/off current ratio of 10$^6$ were observed. A field-effect hole mobility of 5.8 × 10$^{-4}$ cm$^2$/(V s) and an on/off current ratio of 10$^5$ were observed in P3TPPz OFETs processed from 1,2-dichlorobenzene as derived from the output and transfer characteristics shown in Figure 6. These devices showed typical p-channel OFET characteristics with good source/drain current modulation and well-defined saturation regions. The hole mobility of P3TPPz is lower than that of PTDPPz because the long alkyl chains on the thiophene moieties of P3TPPz are known to adversely affect the carrier mobility.[15]

The much higher ionization potentials (5.68 and 5.42 eV) of PPPzF and P2TPPzF likely means a larger hole injection barrier

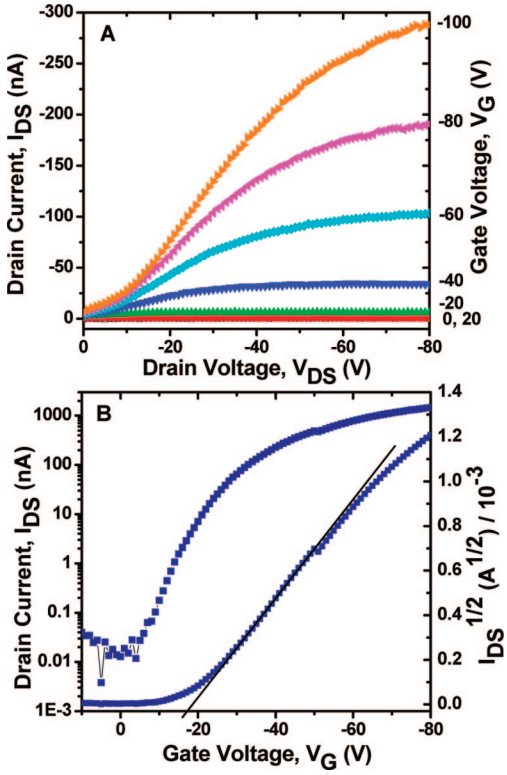


**Figure 5.** Output (A) and transfer (B) characteristics of a PTDPPz field-effect transistor (500 $\mu$m width and 25 $\mu$m channel length) processed from 1,2,4-trichlorobenzene.

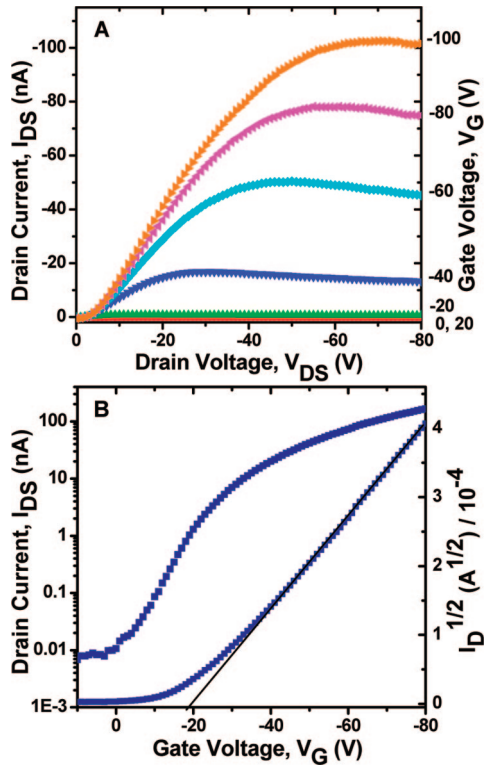


**Figure 6.** Output (A) and transfer (B) characteristics of a P3TPPz field-effect transistor (400 $\mu$m width and 20 $\mu$m channel length) processed from 1,2-dichlorobenzene.

with respect to the gold source/drain electrodes ($\Phi = 5.1$ eV) in the OFETs compared to those (5.20−5.31 eV) of PTHPPz, PTDPPz, and P3TPPz. This may explain why field-effect hole transport characteristics were not observed in PPPzF and P2TPPzF. Although the cyclic voltammograms showed clear ambipolar redox behavior, n-channel OFET characteristics were not observed in any of the copolymer semiconductors. We believe that a major reason why these copolymers did not show ambipolar field-effect charge transport properties is their low electron affinities and thus high electron injection barrier relative to gold source/drain electrodes.

## Conclusions

Soluble pyrido[3,4-*b*]pyrazine-based conjugated donor−acceptor polymer semiconductors with moderate molecular weights were synthesized by Suzuki and Stille coupling polymerizations. The strength of intramolecular charge transfer interaction and thus the electronic and optical properties of the pyrido[3,4-*b*]pyrazine-based copolymers were varied by changing the macromolecular architecture. The copolymers had optical band gaps in the range of 1.75−2.48 eV and ambipolar redox properties with ionization potentials of 5.20−5.68 eV. Among them, PTHPPz, PTDPPz, and P3TPPz with IPs of 5.20−5.31 eV were found to have small charge injection barriers with respect to gold electrodes, which facilitated hole injection and transport in OFETs. The field-effect mobility of holes varied from $5.8 \times 10^{-4}$ cm$^2$/(V s) in P3TPPz thin films to $4.4 \times 10^{-3}$ cm$^2$/(V s) in PTDPPz thin films that both were spin-coated from organic solvents. These results show that soluble pyrido[3,4-*b*]pyrazine-based donor−acceptor copolymer semiconductors combine good charge carrier mobility with broad visible absorption of interest for photovoltaic cells and other optoelectronic applications.

## Experimental Section

**Materials.** All starting materials and reagents were purchased from Aldrich and used without further purification. 5-Tributylstannyl-3-dodecylthiophene,[16] 5,8-dibromo-pyrido[3,4-*b*]pyrazine,[1b] 5,8-dibromo-2,3-diheptylpyrido[3,4-*b*]pyrazine,[1b] 5,8-dibromo-2,3-dioctylpyrido[3,4-*b*]pyrazine,[1b] 5,8-dibromo-2,3-didecylpyrido[3,4-*b*]pyrazine,[1b] and 2,5-bis(trimethylstannyl)thiophene[17] were prepared by modifying the literature methods.

**Poly(pyrido[3,4-*b*]pyrazine-*alt*-9,9-dioctyl-2,7-fluorene) (PPPzF).** To a three-necked flask was added 9,9-dioctylfluorene-2,7-bis(trimethyleneboronate) (313 mg, 0.56 mmol), 5,8-dibromopyrido[3,4-*b*]pyrazine (162 mg, 0.56 mmol), Aliquat 336 (60 mg), and toluene (20 mL). Once the two monomers were dissolved, 2 M aqueous sodium carbonate solution (10 mL) was added. The flask equipped with a condenser was then evacuated and filled with nitrogen several times to remove traces of air. Tetrakis(triphenylphosphine)palladium(0) ($Pd(PPh_3)_4$, 32.4 mg, 0.03 mmol) was then added, and the mixture was stirred for 48 h at 105 °C under argon. The reaction mixture was cooled to room temperature, and the organic layer was separated, washed with water, and precipitated into methanol. The green copolymer sample was filtered, washed with excess methanol, dried, and purified by a Soxhlet extraction with acetone for 2 days (81% yield). $^1$H NMR (300 MHz, $CDCl_3$), $\delta$ (ppm): 9.17 (s, 1H), 9.13 (d, 1H), 9.07 (d, 1H), 8.29 (s, 2H), 8.02−7.84 (m, 4H), 2.16 (b, 4H), 1.18 (b, 20H), 1.02 (b, 4H), 0.82 (b, 6H).

**Poly(thiophene-2,5-diyl-*alt*-2,3-diheptylpyrido[3,4-*b*]pyrazine-5,8-diyl) (PTHPPz).** To a mixture of 5,8-dibromo-2,3-diheptylpyrido[3,4-*b*]pyrazine (485 mg, 1 mmol) and 2,5-bis(trimethylstannyl)thiophene (410 mg, 1 mmol) in dry *N,N*-dimethylformide (DMF, 35 mL) were added $Pd(PPh_3)_4$ (58 mg, 0.05 mmol) as the catalysts. The reaction mixture was stirred at 85 °C under argon for 2 days and precipitated into a mixture of methanol (200 mL) and concentrated hydrochloric acid (5 mL) and stirred for 2 h at room temperature. The precipitate was filtered, washed with excess methanol, and dried. The polymer was purified by a Soxhlet extraction with acetone for 2 days. After drying under vacuum, a dark purple powder of PTHPPz (204 mg, 50%) was obtained. $^1$H NMR (300 MHz, $CF_3COOD$), $\delta$ (ppm): 0.74 (b, 6H), 0.91−2.22

(m, 20H), 3.53 (b, 4H), 8.29 (b, 1H), 8.64 (b, 1H), 9.25 (b, 1H). FT-IR (film, $cm^{-1}$): 3052, 2952, 2922, 2852, 1574, 1524, 1464, 1426, 1392, 1336, 1282, 1172, 1148, 1096, 1054, 1038, 938, 912, 816, 802, 724.

**Poly(thiophene-2,5-diyl-*alt*-2,3-didecylpyrido[3,4-*b*]pyrazine-5,8-diyl) (PTDPPz).** This dark purple copolymer sample was prepared by a procedure similar to that of PTHPPz using 5,8-dibromo-2,3-dideylpyrido[3,4-*b*]pyrazine instead of 5,8-dibromo-2,3-diheptylpyrido[3,4-*b*]pyrazine as the monomer (320 mg, 81% yield). $^1$H NMR (300 MHz, $CF_3COOD$), $\delta$ (ppm): 0.84 (b, 6H), 0.92−1.66 (m, 28H), 2.26 (b, 4H), 3.53 (b, 4H), 8.29 (b, 1H), 8.64 (b, 1H), 9.25 (b, 1H). FT-IR (film, $cm^{-1}$): 3046, 2954, 2922, 2850, 1574, 1524, 1464, 1422, 1392, 1334, 1280, 1168, 1148, 1098, 1054, 1038, 936, 912, 818, 804, 722.

**5,8-Bis(4-dodecylthiophen-2-yl)-2,3-dioctylpyrido[3,4-*b*]pyrazine (1).** To a mixture of 5,8-dibromo-2,3-dioctylpyrido[3,4-*b*]pyrazine (640 mg, 1.25 mmol) and 5-tributylstannylthiophene (1485.2 mg, 2.74 mmol) in dry DMF (35 mL) were added $Pd(PPh_3)_4$ (72 mg, 0.06 mmol) as the catalysts. The reaction mixture was stirred at 85 °C under argon for 2 days. Subsequently, the reaction mixture was poured into 200 mL of water, and the product was extracted with methylene chloride ($CH_2Cl_2$). The organic layer was washed twice with water and dried over anhydrous sodium sulfate. After evaporation of the solvent, the crude product was purified by column chromatography on silica gel (5% ether in hexane as eluent) to yield compound **1** as a orange solid (88%). $^1$H NMR (300 MHz, $CDCl_3$), $\delta$ (ppm): 9.06 (s, 1H), 8.51 (s, 1H), 7.77 (s, 1H), 7.16 (s, 1H), 7.11 (s, 1H), 3.11 (m, 4H), 2.71 (m, 4H), 2.09 (m, 4H), 1.71−1.21 (m, 60H), 0.94 (t, 12H).

**5,8-Bis(5-bromo-4-dodecylthiophen-2-yl)-2,3-dioctylpyrido[3,4-*b*]pyrazine (2).** To a solution of **1** (725 mg, 0.85 mmol) in a mixture of DMF (35 mL) and $CH_2Cl_2$ (35 mL) at room temperature in the dark was added *N*-bromosuccinimide (301 mg, 1.7 mmol) slowly. The resulting solution was stirred for 16 h and then was poured into water (200 mL). The product was extracted with $CH_2Cl_2$. The organic phases were washed with water and dried over sodium sulfate, and the solvent was removed under reduced pressure. The crude product was purified by column chromatography on silica gel (2% ether in hexane) to afford compound **2** (643 mg, 75%) as bright orange solid. $^1$H NMR (300 MHz, $CDCl_3$), $\delta$ (ppm): 9.01 (s, 1H), 8.66 (s, 1H), 7.55 (s, 1H), 3.11 (m, 4H), 2.65 (m, 4H), 2.06 (m, 4H), 1.71−1.28 (m, 60H), 0.91 (t, 12H). MS (ESI mode): Found M + 1, 1015.0, $C_{55}H_{87}Br_2N_3S_2$ requires M, 1014.24.

**Poly(5,8-bis(4-dodecylthiophen-2-yl)-2,3-dioctylpyrido[3,4-*b*]pyrazine-*alt*-2,5-thiophene) (P3TPPz).** This dark purple copolymer sample was prepared by a procedure similar to that of PTHPPz using compound **2** instead of 5,8-dibromo-2,3-diheptylpyrido[3,4-*b*]pyrazine as the monomer and the solvent was toluene instead of DMF (50% yield). $^1$H NMR (300 MHz, $CDCl_3$), $\delta$ (ppm): 9.07 (s, 1H), 8.52 (s, 1H), 7.78 (s, 1H), 7.16 (b, 2H), 2.92−3.11(b, 4H), 2.14−1.28 (b, 58H), 0.88 (b, 12H). FT-IR (film, $cm^{-1}$): 3062, 2952, 2921, 2851, 1533, 1443, 1377, 1275, 1167, 1144, 1114, 910, 865, 832, 787, 721, 696, 659.

**Poly(5,8-bis(4-dodecylthiophen-2-yl)-2,3-dioctylpyrido[3,4-*b*]pyrazine-*alt*-9,9-dioctyl-2,7-fluorene) (P2TPPzF).** This copolymer (45 mg) was prepared by a procedure similar to that of PPPzF using compound **2** (150 mg, 14.8 mmol) instead of 5,8-dibromopyrido[3,4-*b*]pyrazine as the monomer. $^1$H NMR (300 MHz, $CDCl_3$), $\delta$ (ppm): 9.12 (s, 1H), 8.64 (s, 1H), 7.58−7.82 (b, 7H), 3.11−2.81 (b, 8H), 2.14−1.28 (b, 92H), 0.88 (b, 18H).

**Characterization.** $^1$H NMR spectra were recorded on a Bruker-AF300 spectrometer at 300 MHz. Gel permeation chromatography (GPC) analysis of the polymers was performed on a Waters 1515 gel permeation chromatography coupled with UV and RI detectors using tetrahydrofuran as the eluent and polystyrene standards as reference. Thermogravimetric analysis (TGA) analysis was conducted with a TA Instruments Q50 TGA at a heating rate of 10 °C/min under a nitrogen gas flow. UV−vis absorption spectra were recorded on a Perkin-Elmer model Lambda 900 UV/vis/near-IR spectrophotometer. The photoluminescence (PL) emission spectra were obtained with a Photon Technology International (PTI) Inc. model QM-2001-4 spectrofluorimeter. Cyclic voltammetry experiments were done on an EG&G Princeton Applied Research potentiostat/galvanostat (model 273A) in an electrolyte solution of 0.1 M tetrabutylammonium hexafluorophosphate ($Bu_4NPF_6$) in acetonitrile. A three-electrode cell was used in all experiments. Platinum wire electrodes were used as both counter and working electrodes, and silver/silver ion (Ag in 0.1 M $AgNO_3$ solution, Bioanalytical System, Inc.) was used as a reference electrode. The $Ag/Ag^+$ ($AgNO_3$) reference electrode was calibrated at the beginning of the experiments by running cyclic voltammetry on ferrocene as the internal standard. The potential values obtained in reference to $Ag/Ag^+$ electrode were then converted to the saturated calomel electrode (SCE) scale. The films of the polymers were coated onto the Pt working electrode by dipping the Pt wire into a 1 wt % chlorobenzene solution of each copolymer sample and dried under vacuum at 80 °C for 24 h.

**Fabrication and Characterization of Thin-Film Transistors.** Bottom-contact geometry was used to fabricate the thin-film field-effect transistors. Heavily n-doped Si with a conductivity of $10^3$ S/cm was used as a gate electrode with 300 nm thick $SiO_2$ layer as the gate dielectric. Using photolithography and a vacuum deposition system, 60 nm thick gold electrodes (source and drain) with a 10 nm thick adhesive layer of TiW or Cr were patterned onto the $SiO_2$ layer. The $SiO_2$ surfaces of the FET substrates were treated with octyltriethoxysilane (OTS-8) through a vapor deposition. The wafers were placed in a desiccator with a small vial of OTS-8. Then the desiccator was pumped down to vacuum, heated to 80 °C, and left overnight for the deposition of the OTS-8 SAM on the $SiO_2$ surface. After deposition, the FET substrates were sonicated for 1 min in anhydrous toluene. Thin films of the pyrido[3,4-*b*]pyrazine-based D−A copolymers were made by spin-coating a polymer solution onto the OTS-modified $SiO_2$ surface and dried for 10−12 h under vacuum. The gate electrode launching pad was placed on top of the Si gate electrode after the $SiO_2$ gate dielectric had been mechanically etched away. Electrical characteristics of the devices were measured after annealing them at 100 °C for 10 min by using a Keithley 4200 semiconductor parameter analyzer (Keithley Instruments, Inc., Cleveland, OH). All the measurements were done under ambient laboratory conditions.

**Acknowledgment.** This research was supported by the NSF, the AFOSR EHSS MURI (Grant FA9550-06-1-0326), and the DOE BES (DE-FG02-07ER46467).

## References and Notes

(1) (a) Karikomi, M.; Kitamura, C.; Tanaka, S.; Yamashita, Y. *J. Am. Chem. Soc.* **1995**, *117*, 6791. (b) Lee, B.-L.; Yamamoto, T. *Macromolecules* **1999**, *32*, 1375. (c) Yamamoto, T.; Zhou, Z. H.; Kanbara, T.; Shimura, M.; Kizu, K.; Maruyama, T.; Nakamura, Y.; Fukuda, T.; Lee, B.-L.; Ooba, N.; Tomaru, S.; Kurihara, T.; Kaino, T.; Kubota, K.; Sasaki, S. *J. Am. Chem. Soc.* **1996**, *118*, 10389. (d) Zhang, Q. T.; Tour, J. M. *J. Am. Chem. Soc.* **1998**, *120*, 5355. (e) Jenekhe, S. A.; Lu, L.; Alam, M. M. *Macromolecules* **2001**, *34*, 7315. (f) van Mullekom, H. A. M.; Vekemans, J. A. J. M.; Havinga, E. E.; Meijer, E. W. *Mater. Sci. Eng. R.* **2001**, *32*, 1.

(2) (a) Agrawal, A. K.; Jenekhe, S. A. *Macromolecules* **1993**, *26*, 895. (b) Hancock, J. M.; Gifford, A. P.; Champion, R. D.; Jenekhe, S. A. *Macromolecules* **2008**, *41*, 3588. (c) Agrawal, A. K.; Jenekhe, S. A. *Chem. Mater.* **1996**, *8*, 579. (d) Cui, Y.; Zhang, X.; Jenekhe, S. A. *Macromolecules* **1999**, *32*, 3824. (e) Zhu, Y.; Yen, C.-T.; Jenekhe, S. A.; Chen, W.-C. *Macromol. Rapid Commun.* **2004**, *25*, 1829.

(3) (a) Gunes, S.; Neugebauer, H.; Sariciftci, N. S. *Chem. Rev.* **2007**, *107*, 1324. (b) Coakley, K. M.; McGehee, M. D. *Chem. Mater.* **2004**, *16*, 4533. (c) Alam, M. M.; Jenekhe, S. A. *Chem. Mater.* **2004**, *16*, 4647. (d) Sonmez, G.; Shen, C. K. F.; Rubin, Y.; Wudl, F. *Adv. Mater.* **2005**, *17*, 897. (e) Campos, L. M.; Tontcheva, A.; Günes, S.; Sonmez, G.; Neugebauer, H.; Sariciftci, N. S.; Wudl, F. *Chem. Mater.* **2005**, *17*, 4031. (f) Svensson, M.; Zhang, F.; Veenstra, S. C.; Verhees, W. J. H.; Hummelen, J. C.; Kroon, J. M.; Inganäs, O.; Andersson, M. R. *Adv. Mater.* **2003**, *15*, 988. (g) Admassie, S.; Inganäs, O.; Mammo, W.; Perzon, E.; Andersson, M. R. *Synth. Met.* **2006**, *156*, 614. (h) Xin, H.; Kim, F. S.; Jenekhe, S. A. *J. Am. Chem. Soc.* **2008**, *130*, 5424. (i) Blouin, N.; Michaud, A.; Gendron, D.; Wakim, S.; Blair, E.; Neagu-Plesu, R.; Belletete, M.; Durocher, G.; Tao, Y.; Leclerc,

M. *J. Am. Chem. Soc.* **2008**, *130*, 732. (j) Yu, G.; Gao, J.; Hummelen, J. C.; Wudl, F.; Heeger, A. J. *Science* **1995**, *270*, 1789. (k) Jenekhe, S. A.; Yi, S. *Appl. Phys. Lett.* **2000**, *77*, 2635.

(4) (a) Zhang, X.; Jenekhe, S. A. *Macromolecules* **2000**, *33*, 2069. (b) Kulkarni, A. P.; Zhu, Y.; Jenekhe, S. A. *Macromolecules* **2005**, *38*, 1553. (c) Ego, C.; Marsitzky, D.; Becker, S.; Zhang, J.; Grimsdale, A. C.; Müllen, K.; MacKenzie, J. D.; Silva, C.; Friend, R. H. *J. Am. Chem. Soc.* **2003**, *125*, 437. (d) Wu, W.-C.; Liu, C.-L.; Chen, W.-C. *Polymer* **2006**, *47*, 527. (e) Thompson, B. C.; Madrigal, L. G.; Pinto, M. R.; Kang, T.-S.; Schanze, K. S.; Reynolds, J. R. *J. Polym. Sci., Part A: Polym. Chem.* **2005**, *43*, 1417. (f) Hancock, J. M.; Gifford, A. P.; Zhu, Y.; Lou, Y.; Jenekhe, S. A. *Chem. Mater.* **2006**, *18*, 4924. (g) Karastatiris, P.; Mikroyannidis, J. A.; Spiliopoulos, I. K. *J. Polym. Sci., Part A: Polym. Chem.* **2008**, *46*, 2367. (h) Park, M.-J.; Lee, J.; Park, J.-H.; Lee, S. K.; Lee, J.-I.; Chu, H.-Y.; Hwang, D.-H.; Shim, H.-K. *Macromolecules* **2008**, *41*, 3063.

(5) (a) Zhu, Y.; Champion, R. D.; Jenekhe, S. A. *Macromolcules* **2006**, *39*, 8712. (b) Champion, R. D.; Cheng, K.-F.; Pai, C.-L.; Chen, W.-C.; Jenekhe, S. A. *Macromol. Rapid Commun.* **2005**, *26*, 1835. (c) Babel, A.; Wind, J. D.; Jenekhe, S. A. *Adv. Funct. Mater.* **2004**, *14*, 891. (d) Yamamoto, T.; Yasuda, T.; Sakai, Y.; Aramaki, S. *Macromol. Rapid Commun.* **2005**, *26*, 1214. (e) Yamamoto, T.; Kokubo, H.; Kobashi, M.; Sakai, Y. *Chem. Mater.* **2004**, *16*, 4616. (f) Chen, M.; Crispin, X.; Perzon, E.; Andersson, M. R.; Pullerits, T.; Andersson, M.; Inganäs, O.; Berggren, M. *Appl. Phys. Lett.* **2005**, *87*, 252105. (g) Yasuda, T.; Sakai, Y.; Aramaki, S.; Yamamoto, T. *Chem. Mater.* **2005**, *17*, 6060. (h) Pang, H.; Skabara, P.; Crouch, D. J.; Duffy, W.; Heeney, M.; McCulloch, I.; Coles, S. J.; Horton, P. N.; Hursthouse, M. B. *Macromolecules* **2007**, *40*, 6585. (i) Yamamoto, T.; Watanabe, S.; Fukumoto, H.; Sato, M.; Tanaka, T. *Macromol. Rapid Commun.* **2006**, *27*, 317. (j) Babel, A.; Zhu, Y.; Cheng, K.-F.; Chen, W.-C.; Jenekhe, S. A. *Adv. Funct. Mater.* **2007**, *17*, 2542.

(6) (a) Kline, R. J.; McGehee, M. D.; Kadnikova, E. N.; Liu, J.; Fréchet, J. M. J.; Toney, M. F.*Macromolecules* **2005**, *38*, 3312. (b) Zen, A.; Saphiannikova, M.; Neher, D.; Grenzer, J.; Grigorian, S.; Pietsch, U.; Asawapirom, U.; Janietz, S.; Scherf, U.; Lieberwirth, I.; Wegner, G. *Macromolecules* **2006**, *39*, 2162.

(7) (a) Zhang, F.; Jonforsenb, M.; Johanssonb, D. M.; Anderssonb, M. R.; Inganäs, O. *Synth. Met.* **2003**, *138*, 555. (b) Jonforsenb, M.; Zhang, F.; Johanssonb, D. M.; Spjuth, L.; Inganäs, O.; Andersson, M. R. *Synth. Met.* **2002**, *131*, 53.

(8) (a) Chen, T. A.; Wu, X.; Rieke, R. D. *J. Am. Chem. Soc.* **1995**, *117*, 233. (b) Babel, A.; Jenekhe, S. A. *J. Phys. Chem. B* **2003**, *107*, 1749.

(9) (a) Jenekhe, S. A.; Osaheni, J. A. *Science* **1994**, *265*, 765. (b) Osaheni, J. A.; Jenekhe, S. A. *Macromolecules* **1994**, *27*, 739.

(10) (a) Yang, C. J.; Jenekhe, S. A. *Macromolecules* **1995**, *28*, 1180. (b) Kulkarni, A. P.; Tonzola, C. J.; Babel, A.; Jenekhe, S. A. *Chem. Mater.* **2004**, *16*, 4556.

(11) Sariciftci, N. S. *Primary Photoexcitations in Conjugated Polymers: Molecular Excitons vs Semiconductor Band Model*; World Scientific: Singapore, 1997.

(12) (a) Babel, A.; Jenekhe, S. A. *J. Am. Chem. Soc.* **2003**, *125*, 13656. (b) Zhu, Y.; Babel, A.; Jenekhe, S. A. *Macromolecules* **2005**, *38*, 7983. (c) Babel, A.; Jenekhe, S. A. *Macromolecules* **2003**, *36*, 7759. (d) Liao, L. S.; Fung, M. K.; Lee, C. S.; Lee, S. T.; Inbasekaran, M.; Woo, E. P.; Wu, W. W. *Appl. Phys. Lett.* **2000**, *76*, 3582.

(13) Sze, S. M. *Physics of Semiconductor Devices*; Wiley: New York, 1981.

(14) Salleo, A.; Chabinyc, M. L.; Yang, M. S.; Street, R. A. *Appl. Phys. Lett.* **2002**, *81*, 4383.

(15) Babel, A.; Jenekhe, S. A. *Synth. Met.* **2005**, *148*, 169.

(16) Xia, Y.; Deng, X.; Wang, L.; Li, X.; Zhu, X.; Cao, Y. *Macromol. Rapid Commun.* **2006**, *27*, 1260.

(17) van Pham, C.; Macomber, R. S., Jr.; Zimmer, H. *J. Org. Chem.* **1984**, *49*, 5250.

MA801348B